Binary mask optimization for forward lithography based on boundary layer model in coherent systems: erratum

Xu Ma* **and Gonzalo R. Arce**

Department of Electrical and Computer Engineering, University of Delaware, Newark, Delaware 19716, USA
**Corresponding author: maxu@udel.edu*

Received November 17, 2009; accepted November 17, 2009;
posted November 17, 2009 (Doc. ID 119844); published December 9, 2009

This erratum is to correct an error in the simulations detailed in our paper [J. Opt. Soc. Am A **26**, 1687 (2009)].
© 2009 Optical Society of America
OCIS codes: 220.3740, 100.3190, 110.1650.

In [1], we presented simulations to illustrate the characteristics of the proposed binary mask optimization algorithm. However, an error was made in the aerial image calculation. In addition, the range of the point-spread function was overly truncated. We would like to correct these errors and modify the previous simulations in this erratum. The correct simulations are illustrated as follows.

The desired aerial image is shown in Fig. 1. In Fig. 1, p is the pitch width. For the first type of optical lithography system, $p=223.2$ nm on the wafer, and the system parameters are $NA=0.68$ and $\lambda=248$ nm. Since the system is a 4× projection system, the pitch width of the initial interior transmission area pattern $\tilde{\Gamma}$ on the mask is $892.8\ \text{nm}=4\times p$. In the simulation, the mask pattern has the dimensions $2.23\ \mu\text{m}\times 2.23\ \mu\text{m}$. The pixel size is $24.8\ \text{nm}\times 24.8\ \text{nm}$. The convolution kernel is

$$h(\mathbf{r})=\frac{J_1(2\pi rNA/\lambda)}{2\pi rNA/\lambda}, \qquad (1)$$

which is assumed to vanish outside the area A_{h1} defined by $x,y\in[-1.5\ \mu\text{m},1.5\ \mu\text{m}]$. The parameters of the optimization algorithm are $K=L=8$. K is the size of the changeable block, which is described in *Definition 6* in [1]. L is the parameter used to define the type I singular pixel, which is described in *Definition 3* in [1]. The simulation results for the first type of optical lithography system are shown in Fig. 2. The top row (from left to right) shows the initial mask pattern and the corresponding output aerial image, with output pattern error of 1200.1. The error metric is defined as the square of the l^2-norm of the difference between the aerial image and the desired pattern. The middle row (from left to right) shows the optimized binary mask $\tilde{M}'$ based on a thin-mask approximation and the corresponding output aerial image, with output pattern error of 1039.4. The bottom row (from left to right) shows the optimized binary mask based on the boundary layer (BL) model and the corresponding output aerial image, with output pattern error of 972.3. In the mask patterns, black and white represent 0 and 1, respectively. It is shown that the optimization of the binary mask based on the thin-mask approximation reduces the output pattern error by 13.4%. On the other hand, the algorithm based on the BL model reduces the output pattern error by 19.0%. Figure 3 illustrates the intersections of the aerial images on the 45th row. The solid, dashed, and dotted curves represent the intersections corresponding to the initial mask, the optical proximity correction (OPC) based on the thin-mask assumption, and the OPC based on the thick-mask assumption, respectively.

For the second type of optical lithography system, $p=137.8$ nm on the wafer, the system parameters are $NA=0.85$ and $\lambda=193$ nm. The pitch width of the initial interior transmission area pattern $\tilde{\Gamma}$ on the mask is $551.0\ \text{nm}=4\times p$. In the simulation, the mask pattern has the dimensions $1.38\ \mu\text{m}\times 1.38\ \mu\text{m}$. The pixel size is $14.5\ \text{nm}\times 14.5\ \text{nm}$. The convolution kernel is assumed to vanish outside the area A_{h2} defined by $x,y\in[-1.0\ \mu\text{m},1.0\ \mu\text{m}]$. The parameters of the optimization algorithm are $K=L=12$. The simulations results for the second type of optical lithography system are shown in Fig. 4. The top

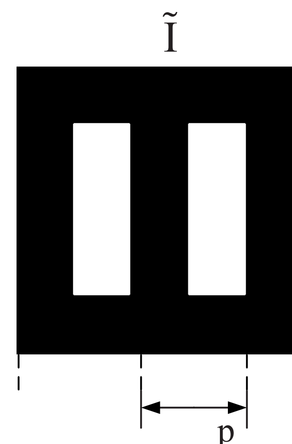

Fig. 1. Desired pattern of the aerial image searched on the wafer.

 © 2010 Optical Society of America

M^* $T\{M^*\}$

Pattern Error=1200.1

$\hat{M}'$ $T\{\hat{M}'\}$

Pattern Error=1039.4

$\hat{M}$ $T\{\hat{M}\}$

Pattern Error=972.3

Fig. 2. OPC optimization based on the BL model for the first type of coherent optical lithography system. $NA=0.68$ and $\lambda=248$ nm. Top row (from left to right), initial mask pattern and corresponding output aerial image; middle row (from left to right), optimized binary mask based on the thin-mask approximation and corresponding output aerial image; bottom row (from left to right), optimized binary mask based on the BL model and corresponding output aerial image. In the mask patterns, black and white represent 0 and 1, respectively.

M^* $T\{M^*\}$

Pattern Error=1352.4

$\hat{M}'$ $T\{\hat{M}'\}$

Pattern Error=1135.9

$\hat{M}$ $T\{\hat{M}\}$

Pattern Error=1089.6

Fig. 4. OPC optimization based on the BL model for the second type of coherent optical lithography system. $NA=0.85$ and $\lambda=193$ nm. Top row (from left to right), initial mask pattern and corresponding output aerial image; middle row (from left to right), optimized binary mask based on the thin-mask approximation and corresponding output aerial image; bottom row (from left to right), optimized binary mask based on the the BL model and corresponding output aerial image. In the mask patterns, black and white represent 0 and 1, respectively.

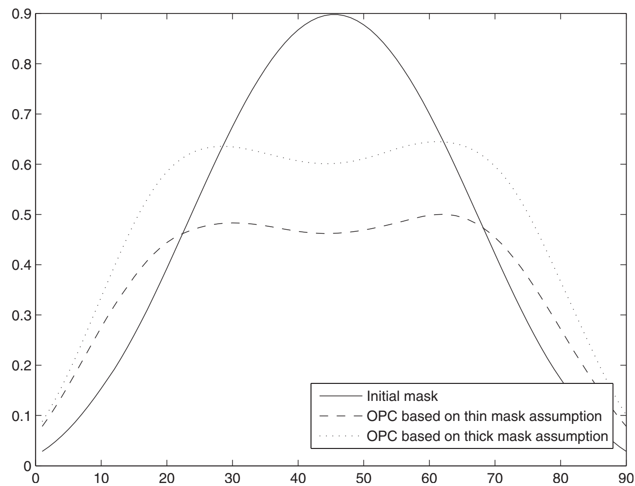

Fig. 3. Intersections of the aerial images shown in Fig. 2 on the 45th row.

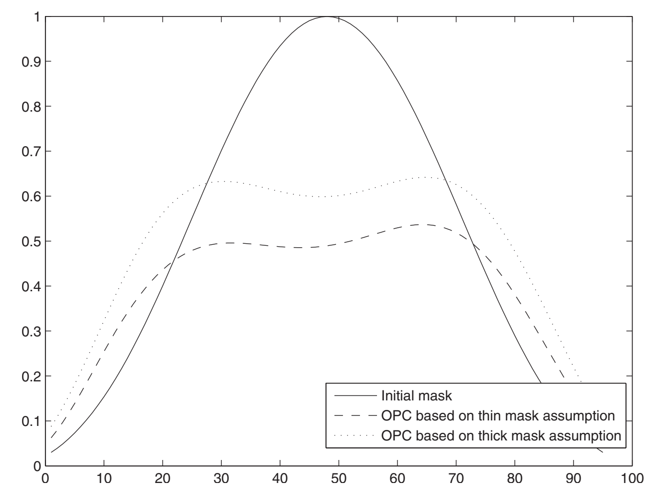

Fig. 5. Intersections of the aerial images shown in Fig. 4 on the 48th row.

row (from left to right) shows the initial mask pattern and the corresponding output aerial image, with output pattern error of 1352.4. The middle row (from left to right) shows the optimized binary mask $\tilde{M}'$ based on the thin-mask approximation and the corresponding output aerial image, with output pattern error of 1135.9. The bottom row (from left to right) shows the optimized binary mask based on the BL model and the corresponding output aerial image, with output pattern error of 1089.6. In the mask patterns, black and white represent 0 and 1, respectively. It is shown that optimization of the binary mask based on the thin-mask approximation reduces the output pattern error by 16.0%. On the other hand, the algorithm based on the BL model reduces the output pattern error by 19.4%. Figure 5 illustrates the intersections of the aerial images on the 48th row. The solid, dashed, and dotted curves represent the intersections corresponding to the initial mask, the OPC based on the thin-mask assumption, and OPC based on the thick-mask assumption, respectively. As shown in Figs. 2 and 4, the described OPC optimization algorithm effectively reduces the output pattern errors and obtains more desirable aerial images. The performance differences between optimizing a mask based on the thin-mask approximation and the BL model show the necessity of the described algorithms taking into account the thick-mask effect.

REFERENCE

1. X. Ma and G. R. Arce, "Binary mask optimization for forward lithography based on the boundary layer model in coherent systems," J. Opt. Soc. Am. A **26**, 1687–1695 (2009).